

# Low-temperature anomaly and anisotropy of critical magnetic fields in transition-metal dichalcogenide superconductors

Tomoya Sano,<sup>1</sup> Kota Tabata,<sup>1</sup> Akihiro Sasaki,<sup>1</sup> and Yasuhiro Asano<sup>1</sup>

<sup>1</sup>*Department of Applied Physics, Hokkaido University, Sapporo 060-8628, Japan*

(Dated: January 29, 2026)

We clarify why spin-singlet superconductivity persists in monolayer transition-metal dichalcogenides even in high magnetic fields beyond the Pauli limit. The phenomenon called Ising protection is caused by two magnetically active potentials: a Zeeman field and an Ising spin-orbit interaction. These potentials induce two spin-triplet pairing correlations in a spin-singlet superconductor. One belonging to odd-frequency symmetry class arises solely from a Zeeman field and always makes the superconducting state unstable. The other belonging to even-frequency symmetry class arise from the interaction between the two magnetic potentials and eliminate the instability caused by odd-frequency pairs. The presence or absence of even-frequency spin-triplet pairs explains the anisotropy of the Ising protection. The analytical expression of the superfluid weight enables us to conclude that even-frequency spin-triplet Cooper pairs support spin-singlet superconductivity in high Zeeman fields.

## I. INTRODUCTION

Superconductivity is quenched by an external magnetic field in two ways: orbital effect fluctuates the phase of superconducting condensate and spin Zeeman effect breaks a spin-singlet Cooper pair. In monolayer transition metal dichalcogenide (TMD) superconductors such as  $\text{MoS}_2$ ,  $\text{NbSe}_2$ ,  $\text{TaS}_2$  [1–4], the orbital effects are negligible for a magnetic field applied parallel to the monolayer. The critical magnetic field in such a case is limited only by the Zeeman effect and its value at zero temperature is called Pauli limit  $H_p$  [5, 6]. In experiments, however, observed critical fields tend to go over the Pauli limit in various superconductors (SCs) such as a thin film [7], organic SCs [8, 9], noncentrosymmetric SCs [10–12], and TMDs [13, 14]. Theories have shown that the spin-orbit interactions (SOIs) weaken the pair-breaking effect by a Zeeman field [7, 15, 16]. In TMDs, the Ising-type SOI locks spin of an electron along the perpendicular direction to the monolayer [17]. A spin-singlet pair consisting of such two electrons seems to robust under Zeeman field parallel to the monolayer. This phenomenon is called Ising protection of superconductivity in recent contexts. The experiments on various SCs [8–14, 17] have also suggested that the Ising protection tends to be stronger at lower temperatures. Although existing theories reproduce such tendency in  $H$ - $T$  phase diagrams [1, 18], there is no satisfactory explanation for the low-temperature anomaly in the Ising protection. In addition, the remarkable anisotropy of the Ising protection has not yet been well understood. The purpose of this paper is to provide a physical picture that fully explains these characteristics of the phenomenon.

The concept of odd-frequency Cooper pairing was first introduced to explain superfluidity of  $^3\text{He}$  [19]. The presence of an odd-frequency Cooper pair was confirmed in proximity structures such as a ferromagnet attached to a SC and at a surface of unconventional SCs [20, 21]. In these cases, odd-frequency pairs appear only locally as

a subdominant superconducting pairing correlation and they do not form any pair potentials. However, they cause unusual phenomena such as the anomalous surface impedance of superconducting proximity structures [22] and the paramagnetic response of small unconventional SCs [23]. Such effects can be explained well by the paramagnetic response of odd-frequency Cooper pairs to external magnetic fields. Odd-frequency Cooper pairs exist also in a uniform superconducting condensate when an electron has extra degree of freedom such as bands [24], orbitals, spins, and sublattices. As odd-frequency Cooper pairs decrease the superfluid density, they decrease the transition temperature to superconducting phase [25–27]. In this paper, we will show that the paramagnetic property of odd-frequency Cooper pairs explains well the low-temperature anomaly of critical magnetic fields and the anisotropy of the Ising protection.

In monolayer TMDs, an electron has an extra internal degree of freedom called as valleys, which enables an extra symmetry option in a pair correlation function in addition to the conventional three symmetry options: frequency, spin-structure, and momentum-parity. The parity of a pairing function under the interchange of the valley indices also characterizes the symmetry of a Cooper pair. We analytically solve the Gor'kov equation for the Bogoliubov-de Gennes Hamiltonian which describes the superconducting states in the presence of such an extra internal degree of freedom of an electron. The symmetry of Cooper pairs are discussed by using the analytical expression of the anomalous Green's function. The transition temperature is obtained by solving the gap equation numerically. In spin-singlet SCs, a Zeeman field always makes the superconducting state unstable because it generates odd-frequency spin-triplet Cooper pairs and decreases the superfluid density. Ising SOI generates an extra pairing correlation that belongs to even-frequency spin-triplet odd-valley symmetry class. We will conclude that such Cooper pairs remove the instability of superconductivity due to a Zeeman field alone. The anisotropy of the Ising protection is characterized by the presence

or absence of the extra pair correlation.

This paper is organized as follows. We explain our theoretical model and provide the analytical expression of the anomalous Green's function in Sec. II. The gap equation and  $H$ - $T$  phase diagram are presented in Sec. III. We discuss the superfluid density in Sec. IV. In Sec. V, we discuss the influences of Rashba SOI and impurities involving SOI on the critical fields. The conclusion is given in Sec. VI. We use the unit of  $k_B = \hbar = c = 1$ , where  $k_B$  is the Boltzmann constant and  $c$  is the speed of light.

## II. MODEL

In typical TMDs, the Fermi surfaces surround  $K$  and  $K'$  points in the Brillouin zone [1–3]. We describe such two Fermi surfaces in terms of two valleys. The normal state Hamiltonian is given by

$$\check{H}_N(\mathbf{k}) = \hat{\xi}_k \hat{\sigma}_0 + \boldsymbol{\beta} \cdot \hat{\boldsymbol{\sigma}} \hat{\rho}_z + \mu_B \mathbf{H} \cdot \hat{\boldsymbol{\sigma}} \hat{\rho}_0, \quad (1)$$

$$\hat{\xi}_k = \frac{1}{2m} (\mathbf{k} \hat{\rho}_0 - \mathbf{K} \hat{\rho}_z)^2 - \mu, \quad (2)$$

where  $\mu$  is the chemical potential,  $\mathbf{K}$  is a vector connecting  $K$  and  $\Gamma$  points, and  $\mathbf{H}$  represents a Zeeman field with  $\mu_B$  being the Bohr magneton. The Pauli matrices in spin and valley spaces are denoted by  $\hat{\boldsymbol{\sigma}} = (\hat{\sigma}_x, \hat{\sigma}_y, \hat{\sigma}_z)$  and  $\hat{\boldsymbol{\rho}} = (\hat{\rho}_x, \hat{\rho}_y, \hat{\rho}_z)$ , respectively. The unit matrices in the two spaces are denoted by  $\hat{\sigma}_0$  and  $\hat{\rho}_0$ . We assume that the SOI  $\boldsymbol{\beta}$  is independent of  $\mathbf{k}$  and changes its sign in the two valleys. The time-reversal operation in such model is given by  $\mathcal{T} = i\hat{\sigma}_y \hat{\rho}_x \mathcal{K}$ , where  $\mathcal{K}$  means the complex conjugation plus  $\mathbf{k} \rightarrow -\mathbf{k}$ . The particle-hole conjugation is represented by  $\check{H}_N(\mathbf{k}) = \check{H}_N^*(-\mathbf{k})$  as usual. Two electrons at the different valleys form a spin-singlet  $s$ -wave Cooper pair. The pair potential for such a pair is represented as

$$\check{\Delta} = \Delta i \hat{\sigma}_y \hat{\rho}_x. \quad (3)$$

We solve the Gor'kov equation for the Bogoliubov-de Gennes Hamiltonian

$$[i\omega_n - H_{\text{BdG}}(\mathbf{k})] \begin{bmatrix} \check{\mathcal{G}} & \check{\mathcal{F}} \\ -\check{\mathcal{F}} & -\check{\mathcal{G}} \end{bmatrix}_{(\mathbf{k}, \omega_n)} = 1, \quad (4)$$

$$H_{\text{BdG}}(\mathbf{k}) = \begin{bmatrix} \check{H}_N(\mathbf{k}) & \check{\Delta} \\ -\check{\Delta} & -\check{H}_N(\mathbf{k}) \end{bmatrix}, \quad (5)$$

where  $\omega_n = (2n + 1)\pi T$  is a Matsubara frequency with  $T$  being a temperature. The Hamiltonian is block-diagonalized into two particle-hole spaces. An electron around  $K$  and a hole around  $K'$  are coupled in one particle-hole space, while an electron around  $K'$  and a hole around  $K$  are coupled in the other. The exact solution of the Gor'kov equation is given in Appendix A.  $\mathbf{K} \hat{\rho}_z$  represents the shift of the band bottom from  $\Gamma$  point to  $K$  and  $K'$  points. As shown in Appendix A, the shift of the wavenumber by  $\mathbf{K}$  does not affect the stability of the superconducting states because the shift is absorbed

by changing the range of the summation over  $\mathbf{k}$ . In what follows, we neglect  $\mathbf{K}$  in the dispersion and discuss the symmetry of Cooper pairs. The anomalous Green's function is given by

$$\begin{aligned} \check{\mathcal{F}}(\mathbf{k}, \omega_n) = \hat{Z}^{-1} & \left[ -(\xi_k^2 + \omega_n^2 + \Delta^2 + \boldsymbol{\beta}^2 - \mu_B^2 \mathbf{H}^2) \hat{\sigma}_0 \right. \\ & + 2 \xi_k \boldsymbol{\beta} \cdot \hat{\boldsymbol{\sigma}} \hat{\rho}_z + 2i \omega_n \mu_B \mathbf{H} \cdot \hat{\boldsymbol{\sigma}} \\ & \left. + 2i (\boldsymbol{\beta} \times \mu_B \mathbf{H}) \cdot \hat{\boldsymbol{\sigma}} \hat{\rho}_z \right] \Delta (i\hat{\sigma}_y) \hat{\rho}_x, \end{aligned} \quad (6)$$

$$\begin{aligned} \hat{Z} = & (\xi_k^2 + \omega_n^2 + \Delta^2 + \boldsymbol{\beta}^2 - \mu_B^2 \mathbf{H}^2)^2 \\ & - 4(i\omega_n \mu_B \mathbf{H} + \xi_k \boldsymbol{\beta} \hat{\rho}_z)^2 + 4\mu_B^2 (\boldsymbol{\beta} \times \mu_B \mathbf{H})^2. \end{aligned} \quad (7)$$

There are four symmetry options for a Cooper pair in the present model: frequency, spin configuration, momentum parity, and valley parity. In the presence of in-plane magnetic field ( $\mathbf{H} \parallel \mathbf{x}$  or  $\mathbf{y}$ ) and the Ising SOI ( $\boldsymbol{\beta} \parallel \mathbf{z}$ ), the two vectors are perpendicular to each other, (i.e.,  $\boldsymbol{\beta} \perp \mathbf{H}$ ). In such a case, four types of pairing correlation exist in a SC as summarized in Table I. The first term in Eq. (6) represents the pairing correlation that belongs to even-frequency spin-singlet  $s$ -wave even-valley symmetry and is linked to the pair potential through the gap equation. The SOI generates the pairing correlation at the second term which belongs to even-frequency spin-triplet  $s$ -wave odd-valley symmetry. Such even-frequency Cooper pairs always stabilize the superconducting states in a spin-singlet superconductor. This term explains of the anisotropic magnetic susceptibility in noncentrosymmetric SCs [28] and the Josephson coupling of a spin-singlet SC to a spin-triplet SC [29]. The third term represents the pairing correlation belonging to odd-frequency spin-triplet  $s$ -wave even-valley symmetry. Such odd-frequency pairs suppress the critical magnetic field because they reduce the superfluid density and make the superconducting state unstable [15, 30, 31]. The last term represents the pairing correlation belonging to even-frequency spin-triplet  $s$ -wave odd-valley symmetry class. The combination between the SOI and a Zeeman field generates this pairing correlation. In the succeeding sections, we will show that difference in the temperature dependence of even- and odd-frequency Cooper pairs leads to an enhancement of the critical magnetic field. For a magnetic configuration  $\boldsymbol{\beta} \parallel \mathbf{H}$ , the last term in Eq. (6) vanishes. As shown in the next section, the critical field in such configuration remains unchanged from that in the absence of the SOI.

## III. GAP EQUATION

We solve the gap equation to obtain the transition temperature and draw the  $H$ - $T$  phase diagram. The gap equation is expressed as

$$\Delta = -\frac{1}{4} g N_0 T \sum_{\omega_n} \int d\xi \text{Tr} [\check{\mathcal{F}}(\xi, \omega_n) (-i\hat{\sigma}_y) \hat{\rho}_x], \quad (8)$$

TABLE I. Symmetry classification of the pair correlation functions. The top row corresponds to the pairing correlation that is linked to the pair potential through the Eq. (8). The SOI generates the pairing correlation at the second row from the top. A Zeeman field induces the two pairing correlations: one belongs to odd-frequency symmetry as shown in the third row and the other belongs to even-frequency symmetry as listed at the bottom row.

frequency	spin ( $\times i\hat{\sigma}_y$ )	parity	valley-parity
even	singlet	even	even $\hat{\rho}_x$
even	triplet $\beta \cdot \hat{\sigma}$	even	odd $\hat{\rho}_y$
odd	triplet $\mathbf{H} \cdot \hat{\sigma}$	even	even $\hat{\rho}_x$
even	triplet $\beta \times \mathbf{H} \cdot \hat{\sigma}$	even	odd $\hat{\rho}_y$
			$q_{\perp}$

where  $g > 0$  represents the short-range attractive interaction between two electrons and  $N_0$  is the density of states at the Fermi level in the normal state.  $\text{Tr}$  meaning the trace taken over spin and valley spaces extracts the spin-singlet valley-even component from the anomalous Green's function. The transition temperature  $T_c$  for  $\beta \perp \mathbf{H}$  is obtained by solving the linearized gap equation

$$\log\left(\frac{T}{T_0}\right) + 2\pi T \sum_{\omega_n > 0} \frac{1}{\omega_n} \left[ 1 - \frac{\omega_n^2 + \beta^2}{\omega_n^2 + \beta^2 + \mu_B^2 H^2} \right] = 0, \quad (9)$$

with  $T = T_c$ , where  $T_0$  is the transition temperature in the absence of a Zeeman field and the SOI. In the limit of strong SOI  $\beta \gg \mu_B H$ , it has been already known that the transition temperature approaches  $T_0$  [2]. The numerical results for the critical Zeeman field  $H_c$  are plotted as a function of temperature in Fig. 1 (a) for several choices of  $\beta$ . The critical field  $H_c$  and a temperature respectively are normalized to  $\Delta_0$  and  $T_0$ , where  $\Delta_0$  denotes the pair potential at  $H = \beta = T = 0$ . At  $\beta = 0$ , the results for  $T < 0.556T_0$  correspond to the first order transition points to the superconducting phase [15, 30]. The arrow at the vertical axis indicates the Pauli limit  $\mu_B H_p = \Delta_0/\sqrt{2}$ . For  $\beta \geq \Delta_0$ , all the results are obtained from the second order transition points to the superconducting phase. The critical fields increase with increasing  $\beta$  in agreement with several previous studies [1–3, 17]. This effect is referred to in recent contexts as the Ising protection of superconductivity. The results in Fig. 1(a) show that the Ising protection becomes stronger at lower temperatures.

For a magnetic configuration of  $\beta \parallel \mathbf{H}$ , the gap equation becomes

$$\Delta = \frac{\Delta}{4} g N_0 T \sum_{\omega_n} \int d\xi \text{Tr} \left[ \hat{Z}_+^{-1} + \hat{Z}_-^{-1} \right], \quad (10)$$

$$\hat{Z}_{\pm} = -(\xi \pm \beta \hat{\rho}_z)^2 + (\omega \pm i\mu_B H)^2 + \Delta^2, \quad (11)$$

as shown in Appendix A. By taking the trace over two valleys and shifting the integration variable as  $\xi \pm \beta \rightarrow \xi$ , the  $\beta$ -dependence is eliminated from the gap equation. At  $\beta \times \mathbf{H} = 0$ , the SOI modifies the band dispersion only

slightly. Therefore, the SOI does not affect the critical field for  $\beta \parallel \mathbf{H}$ . The resulting  $H_c$  is identical to that at  $\beta = 0$  as plotted by a dashed line in Fig. 1 (a). Thus, the magnetic configuration  $\beta \times \mathbf{H}$  is a source of the Ising protection.

The orbital effects due to a magnetic field explains the anisotropy of the Ising protection observed in experiments [1–3, 17]. According to our analysis, the Zeeman effect further enhance the anisotropy. In the next section, we explain mechanisms behind the anisotropy of the Ising protection and its low-temperature anomaly.

#### IV. SUPERFLUID DENSITY

To clarify the mechanism of the anisotropy and the low-temperature anomaly of Ising protection, we analyze the stability of the superconducting states by calculating the superfluid density. The superfluid density is defined as

$$Q = Q_{\mathcal{G}} + Q_{\mathcal{F}}, \quad (12)$$

$$Q_{\mathcal{G}} = \frac{1}{2} n T \sum_{\omega_n} \int d\xi \text{Tr} [\check{\mathcal{G}} \check{\mathcal{G}} - \check{\mathcal{G}}^N \check{\mathcal{G}}^N]_{(\mathbf{k}, \omega_n)}, \quad (13)$$

$$Q_{\mathcal{F}} = \frac{1}{2} n T \sum_{\omega_n} \int d\xi \text{Tr} [-\check{\mathcal{F}} \check{\mathcal{F}}]_{(\mathbf{k}, \omega_n)}, \quad (14)$$

where  $n$  is the electron density per spin and  $\check{\mathcal{G}}^N$  is the Green's function in the normal state. As we find a relation  $Q_{\mathcal{G}} = Q_{\mathcal{F}}$  as a result of the calculation, we discuss how the four pairing correlations in Table I contribute to  $Q_{\mathcal{F}}$ . Since the superfluid density is proportional to  $\Delta^2$ , its temperature dependence is strongly governed by that of the pair potential. Therefore, we evaluate the superfluid weight along the phase transition line in Fig. 1(a) which is defined as

$$q(T) = \frac{Q(H_c(T), T)}{n \Delta^2} \Big|_{\Delta \rightarrow 0}. \quad (15)$$

Here  $H_c(T)$  is determined from the data points on the phase boundary in Fig. 1 (a). From the superfluid weight, we capture the contributions of the even- and odd-frequency Cooper pairs to the superfluid density just below the transition temperature. In the expression of the Ginzburg-Landau free-energy

$$F_{\text{SN}} = a\Delta^2 + b\Delta^4 + \text{h.o.t.}, \quad (16)$$

the left-hand-side of Eq. (9) is proportional to the coefficient  $a$  which is zero at  $T = T_c$  and negative for  $T < T_c$ . The superfluid weight  $q_{\mathcal{F}}$  is proportional to the coefficient  $b$  with the same sign [31]. Therefore, the condition  $q_{\mathcal{F}} > 0$  ensures a second-order transition to the stable superconducting state.

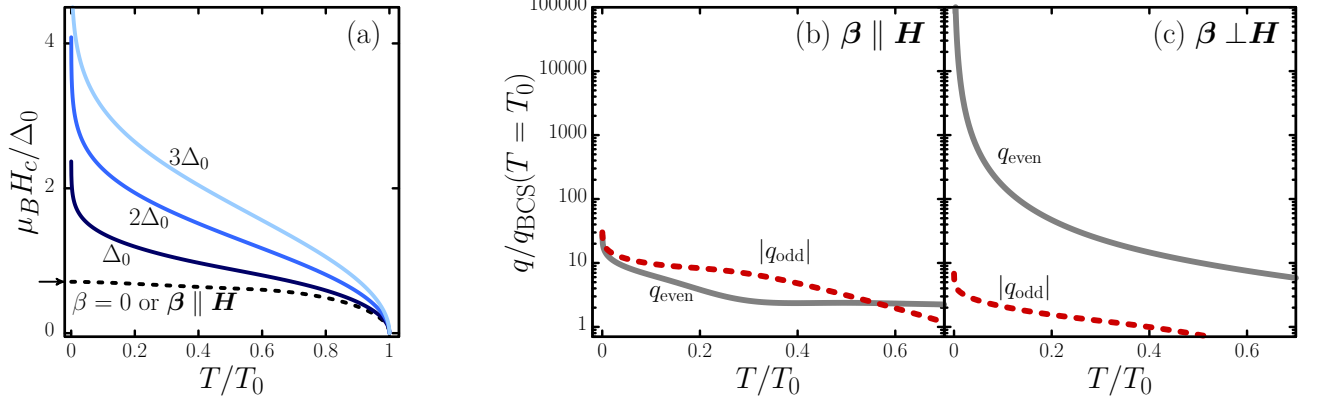


FIG. 1. The critical magnetic field  $H_c$  is plotted as a function of temperature  $T$  for several values of the Ising spin-orbit interactions  $\beta$  in (a). The arrow on the vertical axis indicates the Pauli limit  $\mu_B H_p = \Delta_0/\sqrt{2}$ . The superfluid weights along the transition line in (a) is shown for  $\beta \parallel \mathbf{H}$  in (b) and  $\beta \perp \mathbf{H}$  in (c), where the strength of the Ising SOI is fixed at  $\beta = \Delta_0$ . The critical field  $H_c(T)$  is obtained from the data in (a) for each temperature.

### A. Parallel configuration

We first discuss the parallel configuration  $\beta \parallel \mathbf{H}$  in which the Ising protection is absent as shown in Fig. 1 (a). The superfluid weight consists of two contributions,

$$q_{\mathcal{F}} = q_{\text{even}} + q_{\text{odd}}, \quad (17)$$

$$q_{\text{even}} = 2\pi T \sum_{\omega_n > 0} \frac{2\omega_n^4 - \omega_n^2 \mu_B^2 H_c^2 + \mu_B^4 H_c^4}{2\omega_n(\omega_n^2 + \mu_B^2 H_c^2)^3}, \quad (18)$$

$$q_{\text{odd}} = -2\pi T \sum_{\omega_n > 0} \frac{5\omega_n^2 \mu_B^2 H_c^2 + \mu_B^4 H_c^4}{2\omega_n(\omega_n^2 + \mu_B^2 H_c^2)^3}, \quad (19)$$

where  $q_{\text{even}}$  and  $q_{\text{odd}}$  are the superfluid weight of even- and odd-frequency Cooper pairs, respectively. The superfluid weight of odd-frequency pairs is always negative. The calculated results are plotted in Fig. 1 (b). The superfluid weight of even-frequency spin-singlet  $s$ -wave component  $q_{\text{even}}$  shows a nonmonotonic dependence on temperatures. For  $T < 0.556T_0$ , the amplitude of the odd-frequency component becomes larger than that of the even-frequency component, which leads to  $q_{\mathcal{F}} < 0$ . As a result, the transition to the superconducting state becomes discontinuous [31].

For the latter convenient, we supply the analytical results at low temperatures, where the Matsubara summation is replaced by the integration with a low energy cut-off  $\omega_{\min} = 2\pi T$ . The superfluid weight is calculated to be

$$q_{\text{even/odd}} \approx +/ - \frac{1}{2\mu_B^2 H_c^2} \log \left( \frac{\mu_B H_c}{2\pi T} \right), \quad (20)$$

for  $T \ll \mu_B H$ . Both the weights exhibit a logarithmic dependence on temperature. It would be helpful to compare the results in Eq. (20) with those in the superfluid

weight in BCS theory

$$q_{\text{BCS}} = 2\pi T \sum_{\omega_n > 0} \frac{1}{\omega_n^3} = \frac{1}{2(2\pi T)^2}. \quad (21)$$

The vertical axis in Fig. 1 (b) and (c) is normalized to  $q_{\text{BCS}}$  at  $T = T_0$ . At low temperatures,  $q_{\text{BCS}}$  indicate the power-law dependence on temperature. Thus, the expected relationship  $q_{\text{even}} \ll q_{\text{BCS}}$  also indicates the instability of the superconducting state. A Zeeman field for  $\beta \parallel \mathbf{H}$  reduces the superfluid weight  $q_{\text{even}}$  drastically.

### B. Perpendicular configuration

For  $\beta \perp \mathbf{H}$ , the superfluid weight  $q_{\mathcal{F}}$  consists of the four parts as

$$q_{\mathcal{F}} = q_0 + q_{\beta} + q_{\perp} + q_{\text{odd}}, \quad (22)$$

$$q_0 = 2\pi T \sum_{\omega_n > 0} \frac{1}{z} \left\{ 2\omega_n^6 + \omega_n^4 (5\beta^2 - \mu_B^2 H_c^2) + \omega_n^2 (4\beta^4 + \mu_B^4 H_c^4) + \beta^4 (\beta^2 + \mu_B^2 H_c^2) \right\}, \quad (23)$$

$$q_{\beta} = 2\pi T \sum_{\omega_n > 0} \frac{1}{z} \beta^2 \left( \omega_n^2 + \beta^2 + \mu_B^2 H_c^2 \right)^2, \quad (24)$$

$$q_{\text{odd}} = -2\pi T \sum_{\omega_n > 0} \frac{1}{z} \omega_n^2 \mu_B^2 H_c^2 \left( 5\omega_n^2 + \beta^2 + \mu_B^2 H_c^2 \right), \quad (25)$$

$$q_{\perp} = 2\pi T \sum_{\omega_n > 0} \frac{1}{z} \beta^2 \mu_B^2 H_c^2 \left( 5\omega_n^2 + \beta^2 + \mu_B^2 H_c^2 \right), \quad (26)$$

$$z = 2\omega_n^3 (\omega_n^2 + \beta^2 + \mu_B^2 H_c^2)^3. \quad (27)$$

The first term  $q_0$  is derived from a spin-singlet Cooper pair linked to the pair potential. The terms  $q_{\beta}$  and  $q_{\perp}$  are the contributions of the two even-frequency spin-triplet pairing correlations in Table I. The odd-frequency

pairing correlation  $q_{\text{odd}}$  decrease the superfluid density [22, 23, 25, 31]. We plot the superfluid weights as a function of temperature in Fig. 1 (c). In contrast to the results in Fig. 1 (b), the amplitude of even-frequency components  $q_{\text{even}} = q_0 + q_\beta + q_\perp$  is much larger than  $q_{\text{odd}}$ , which indicates stable superconducting state. The SOI relaxes the instability of the superconducting state due to a Zeeman field for  $\beta \perp \mathbf{H}$ . In particular at  $T = 0$ , the equation  $q_{\text{odd}}/q_{\text{even}} \approx 0$  leads to  $\mu_B H_c \gg \beta$ , which explains the low-temperature anomaly in  $H_c$ .

The source of the Ising protection  $q_{\text{even}} \gg q_{\text{odd}}$  is explained well by the analytical expression of superfluid weights at low temperatures

$$q_{\text{even}} \approx \frac{\mu_B^2 H_c^2}{2(\beta^2 + \mu_B^2 H_c^2)^2} \log \left( \frac{\sqrt{\beta^2 + \mu_B^2 H_c^2}}{2\pi T} \right) + \frac{1}{2} \left[ 1 - \frac{\mu_B^2 H_c^2}{\beta^2 + \mu_B^2 H_c^2} \right] \frac{1}{(2\pi T)^2}, \quad (28)$$

$$q_{\text{odd}} \approx -\frac{\mu_B^2 H_c^2}{2(\beta^2 + \mu_B^2 H_c^2)^2} \log \left( \frac{\sqrt{\beta^2 + \mu_B^2 H_c^2}}{2\pi T} \right). \quad (29)$$

The two superfluid weights exhibit qualitatively different behaviors from each other. Equation (28) shows that  $q_{\text{even}}$  recovers a power-law dependence on temperature as that in  $q_{\text{BCS}}$  as shown in Eq. (21). On the other hand,  $q_{\text{odd}}$  remains a logarithmic dependence. As shown in Eq. (6), the odd-frequency pairing correlation is proportional to the Matsubara frequency  $\omega_n$ . As a result,  $\omega_n^2$  appearing at the numerator of Eq. (25) changes the singularity of the integrand at small  $\omega_n$  from  $\omega_n^{-3}$  to  $\omega_n^{-1}$ . Equations (28) and (25) mathematically express the physics behind the Ising protection of superconducting state.

### C. Intermediate configuration

For intermediate configurations, we only show the numerical results of  $H_c$  at  $T = 0.1T_0$  in Fig. 2, where  $\theta$  is the angle between  $\beta$  and  $\mathbf{H}$ . At  $\theta = 0$  corresponding to the configuration  $\beta \parallel \mathbf{H}$ ,  $H_c$  takes a value near the Pauli limit  $H_p$  independent of  $\beta$ . The critical field increases monotonically with increasing  $\theta$ . At  $\pi/2$  corresponding to  $\beta \perp \mathbf{H}$ ,  $H_c$  becomes larger for larger  $\beta$ .

The shape of curves in Fig. 2 represents the degree of anisotropy solely from the Ising protection. In experiments, however,  $H_c$ - $\theta$  curves influenced by other factors. At  $\theta = 0$ ,  $H_c$  in real TMDs is expected to be smaller than  $H_p$  because the orbital effect due to a magnetic field suppresses superconductivity. The enhancement of  $H_c$  around  $\theta = \pi/2$  depends sensitively on temperature. If the Rashba SOI coexists with the Ising SOI in real TMDs, the Rashba SOI drastically suppresses the enhancement of  $H_c$  around  $\theta = \pi/2$  as briefly discussed in Sec. V.

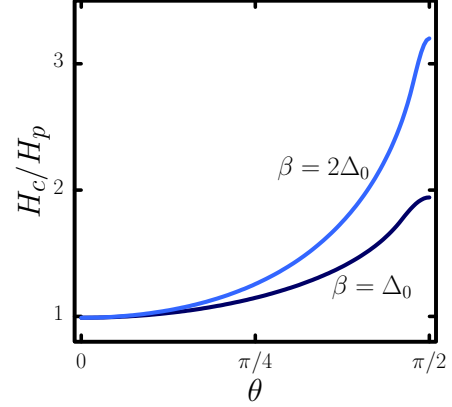


FIG. 2. The critical Zeeman field  $H_c$  at  $T = 0.1T_0$  is plotted as a function of the angle  $\theta$  between  $\beta$  and  $\mathbf{H}$  for two values of the Ising spin-orbit interactions  $\beta$ . The angles  $\theta = 0$  and  $\theta = \pi/2$  correspond to the out-of-plane and in-plane magnetic fields, respectively.

## V. DISCUSSION

The enhancement of the critical field by impurities involving spin-orbit interaction has been established in previous studies [15, 16]. In these studies, impurity self-energy of an electron has the same spin-structure as that of Ising SOI because the motion of an electron is limited within a two-dimensional superconducting layer. Thus, the impurity self-energy is considered to generate pairing correlation that belongs to the same symmetry class as the last term in Eq. (6). In fact, the gap equation for  $T_c$  in the dirty limit takes a similar form to Eq. (9).

The Rashba SOI is another type of spin-orbit interaction. The low-temperature anomaly of  $H_c$  cannot be seen in  $H$ - $T$  phase diagram for a SC with the Rashba SOI [32]. Unlike the Ising SOI, the Rashba SOI has two components: one is perpendicular to the Zeeman field and the other is parallel to the Zeeman field. Although the perpendicular component stabilizes the superconducting state, the parallel component generates additional odd-frequency pairing correlations proportional to

$$i\omega_n \mu_B \mathbf{H} \cdot \beta i\hat{\sigma}_y \hat{\rho}_y, \quad (30)$$

according to Eq. (7). Thus, the perpendicular and parallel components of Rashba SOI exhibit opposite effects on  $H_c$ . A numerical simulation has reported that the Rashba SOI drastically suppresses the low-temperature anomaly of  $H_c$  due to the Ising SOI [1].

## VI. CONCLUSION

We have theoretically investigated the mechanism of the Ising protection of superconducting state in monolayer transition-metal dichalcogenide superconductors

under a Zeeman field parallel to the layer. The following conclusions can be obtained from the analytical expression of the anomalous Green's function and that of the superfluid density. In a spin-singlet superconductor, a Zeeman field  $\mathbf{H}$  always makes the superconducting state unstable because it reduces the superfluid density by breaking the even-frequency Cooper pairs and by generating odd-frequency Cooper pairs. Generally speaking, even-frequency (odd-frequency) Cooper pairs increase (decrease) superfluid density. The Ising spin-orbit interaction  $\beta \perp \mathbf{H}$  drastically increases the superfluid density and relaxes the instability due to a Zeeman field. Such effect is more remarkable in lower

temperatures. However, the Ising spin-orbit interaction  $\beta \parallel \mathbf{H}$  does not change the superfluid density at all. These characteristic behaviors of the superfluid densities explains the anisotropy of the Ising protection and its low-temperature anomaly. Such an anisotropy is explained also by the presence of even-frequency Cooper pairs whose correlation function is proportional to  $\beta \times \mathbf{H}$ .

## ACKNOWLEDGMENTS

T. S. was supported by JST SPRING, Grant Number JPMJSP2119.

## Appendix A: SOLUTION

In this appendix, we show the full BdG Hamiltonian and the Green's functions. The BdG Hamiltonian reads

$$H_{\text{BdG}}(\mathbf{k}) = \begin{bmatrix} \xi_- + \beta \cdot \hat{\sigma} + \mathbf{V} \cdot \hat{\sigma} & 0 & 0 & \Delta i \hat{\sigma}_y \\ 0 & \xi_+ - \beta \cdot \hat{\sigma} + \mathbf{V} \cdot \hat{\sigma} & \Delta i \hat{\sigma}_y & 0 \\ 0 & -\Delta i \hat{\sigma}_y & -\xi_+ - \beta \cdot \hat{\sigma}^* - \mathbf{V} \cdot \hat{\sigma}^* & 0 \\ -\Delta i \hat{\sigma}_y & 0 & 0 & -\xi_- + \beta \cdot \hat{\sigma}^* - \mathbf{V} \cdot \hat{\sigma}^* \end{bmatrix}, \quad (\text{A1})$$

$$\xi_{\pm} = \frac{1}{2m}(\mathbf{k} \pm \mathbf{K})^2 - \mu, \quad \mathbf{V} = \mu_B \mathbf{H}. \quad (\text{A2})$$

The solution of the Gor'kov equation is calculated as

$$\check{\mathcal{G}}(\mathbf{k}, \omega_n) = \hat{Z}^{-1} \left[ \left\{ (i\omega_n - \hat{\xi}) \hat{z}_N - (i\omega_n + \hat{\xi}) \Delta^2 \right\} \hat{\sigma}_0 + (\hat{z}_N + \Delta^2) \mathbf{V} \cdot \hat{\sigma} + (\hat{z}_N - \Delta^2) \beta \cdot \hat{\sigma} \hat{\rho}_z \right] \hat{\rho}_0, \quad (\text{A3})$$

$$\check{\mathcal{F}}(\mathbf{k}, \omega_n) = \hat{Z}^{-1} \left[ - \left( \hat{\xi}^2 + \omega_n^2 + \Delta^2 + \beta^2 - \mathbf{V}^2 \right) \hat{\sigma}_0 + 2i\omega_n \mathbf{V} \cdot \hat{\sigma} + 2\hat{\xi} \beta \cdot \hat{\sigma} \hat{\rho}_z - 2i(\mathbf{V} \times \beta) \cdot \hat{\sigma} \hat{\rho}_z \right] \Delta (i\hat{\sigma}_y) \hat{\rho}_x, \quad (\text{A4})$$

$$\hat{Z} = \left( \hat{\xi}^2 + \omega_n^2 + \Delta^2 + \beta^2 - \mathbf{V}^2 \right)^2 - 4 \left( i\omega_n \mathbf{V} + \hat{\xi} \beta \hat{\rho}_z \right)^2 + 4(\mathbf{V} \times \beta)^2, \quad (\text{A5})$$

$$\hat{z}_N = \left( i\omega_n + \hat{\xi} \right)^2 - (\mathbf{V} - \beta \hat{\rho}_z)^2, \quad (\text{A6})$$

$$\hat{\xi} = \begin{bmatrix} \xi_- & 0 \\ 0 & \xi_+ \end{bmatrix}. \quad (\text{A7})$$

The anomalous Green's function for  $\beta \parallel \mathbf{H} \parallel z$  near the transition temperature is represented as

$$\check{\mathcal{F}}(\mathbf{k}, \omega_n) = -\frac{1}{2} \left[ \left\{ (\hat{\xi} - \beta \hat{\rho}_z)^2 + (\omega_n - iV)^2 \right\}^{-1} + \left\{ (\hat{\xi} + \beta \hat{\rho}_z)^2 + (\omega_n + iV)^2 \right\}^{-1} \right. \\ \left. + \left\{ (\hat{\xi} - \beta \hat{\rho}_z)^2 + (\omega_n - iV)^2 \right\}^{-1} \hat{\sigma}_z - \left\{ (\hat{\xi} + \beta \hat{\rho}_z)^2 + (\omega_n + iV)^2 \right\}^{-1} \hat{\sigma}_z \right] \Delta (i\hat{\sigma}_y) \hat{\rho}_x. \quad (\text{A8})$$

The gap equation is composed of the summation of the anomalous Green's function over wavenumbers.

$$\frac{1}{V_{\text{vol}}} \sum_{\mathbf{k}} \check{\mathcal{F}}(\mathbf{k}, \omega_n) = -\frac{1}{2} \frac{1}{V_{\text{vol}}} \sum_{\mathbf{k}} \left[ \left\{ (\xi_{\mathbf{k}} - \beta \hat{\rho}_z)^2 + (\omega_n - iV)^2 \right\}^{-1} + \left\{ (\xi_{\mathbf{k}} + \beta \hat{\rho}_z)^2 + (\omega_n + iV)^2 \right\}^{-1} \right. \\ \left. + \left\{ (\xi_{\mathbf{k}} - \beta \hat{\rho}_z)^2 + (\omega_n - iV)^2 \right\}^{-1} \hat{\sigma}_z - \left\{ (\xi_{\mathbf{k}} + \beta \hat{\rho}_z)^2 + (\omega_n + iV)^2 \right\}^{-1} \hat{\sigma}_z \right] \Delta (i\hat{\sigma}_y) \hat{\rho}_x, \quad (\text{A9})$$

$$= -\frac{1}{2} N_0 \int d\xi \left[ \frac{1}{\xi^2 + (\omega_n - iV)^2} + \frac{1}{\xi^2 + (\omega_n + iV)^2} \right. \\ \left. + \frac{1}{\xi^2 + (\omega_n - iV)^2} \hat{\sigma}_z - \frac{1}{\xi^2 + (\omega_n + iV)^2} \hat{\sigma}_z \right] \Delta (i\hat{\sigma}_y) \hat{\rho}_x, \quad (\text{A10})$$

$$\xi_{\mathbf{k}} = \frac{\mathbf{k}^2}{2m} - \mu. \quad (\text{A11})$$

We shift the wavenumber as  $\mathbf{k} \rightarrow \mathbf{k} \mp \mathbf{K}$  for  $\xi_{\pm}$  to reach Eq. (A9) and change  $\xi \pm \beta \rightarrow \xi$  to reach Eq. (A10). Equation (A10) has exactly the same expression as that for the Green's function in uniform Zeeman field. Thus,  $T_c$  for  $\beta \parallel \mathbf{H}$  is equal to that with  $\beta = 0$ . The first two terms in Eq. (A10) represent even-frequency spin-singlet  $s$ -wave even-valley Cooper pairs. The last two terms are the correlation of odd-frequency spin-triplet  $s$ -wave even-valley Cooper pairs. The two components contribute to the superfluid density in the opposite way as shown in the text.

The anomalous Green's function for  $\beta \parallel z$  and  $\mathbf{H} \parallel y$  near the transition temperature is obtained

$$\frac{1}{V_{\text{vol}}} \sum_{\mathbf{k}} \check{\mathcal{F}}(\mathbf{k}, \omega_n) = -\frac{1}{V_{\text{vol}}} \sum_{\mathbf{k}} \frac{[(\xi_{\mathbf{k}}^2 + \omega^2 + \beta^2 - V^2) + 2i\omega_n V \hat{\sigma}_y + 2\xi_{\mathbf{k}} \beta \hat{\sigma}_z \hat{\rho}_z - 2iV \beta \hat{\sigma}_x \hat{\rho}_z]}{\xi_{\mathbf{k}}^4 + 2\xi_{\mathbf{k}}^2 (\omega_n^2 - \beta^2 - V^2) + (\omega_n^2 + \beta^2 + V^2)^2} \Delta(i\hat{\sigma}_y) \hat{\rho}_x. \quad (\text{A12})$$

Here we have already shifted the wavenumber  $\mathbf{k} \rightarrow \mathbf{k} \mp \mathbf{K}$  for  $\xi_{\pm}$ .

---

[1] Y. Saito, Y. Nakamura, M. S. Bahramy, Y. Kohama, J. Ye, Y. Kasahara, Y. Nakagawa, M. Onga, M. Tokunaga, T. Nojima, *et al.*, Superconductivity protected by spin-valley locking in ion-gated MoS<sub>2</sub>, *Nature Physics* **12**, 144 (2016).

[2] X. Xi, Z. Wang, W. Zhao, J.-H. Park, K. T. Law, H. Berger, L. Forró, J. Shan, and K. F. Mak, Ising pairing in superconducting NbSe<sub>2</sub> atomic layers, *Nature Physics* **12**, 139 (2016).

[3] S. C. De la Barrera, M. R. Sinko, D. P. Gopalan, N. Sivadas, K. L. Seyler, K. Watanabe, T. Taniguchi, A. W. Tsien, X. Xu, D. Xiao, *et al.*, Tuning Ising superconductivity with layer and spin-orbit coupling in two-dimensional transition-metal dichalcogenides, *Nature Communications* **9**, 1427 (2018).

[4] S. Simon, H. Yerzhakov, S. KP, A. Vakahi, S. Remenik, J. Ruhman, M. Khodas, O. Millo, and H. Steinberg, The transition-metal-dichalcogenide family as a superconductor tuned by charge density wave strength, *Nature Communications* **15**, 10439 (2024).

[5] B. Chandrasekhar, A note on the maximum critical field of high-field superconductors, *Appl. Phys. Letters* **1** (1962).

[6] A. M. Clogston, Upper Limit for the Critical Field in Hard Superconductors, *Phys. Rev. Lett.* **9**, 266 (1962).

[7] P. M. Tedrow and R. Meservey, Critical magnetic field of very thin superconducting aluminum films, *Phys. Rev. B* **25**, 171 (1982).

[8] C. C. Agosta, J. Jin, W. A. Coniglio, B. E. Smith, K. Cho, I. Stroe, C. Martin, S. W. Tozer, T. P. Murphy, E. C. Palm, J. A. Schlueter, and M. Kurmoo, Experimental and semiempirical method to determine the Pauli-limiting field in quasi-two-dimensional superconductors as applied to  $\kappa$ -(BEDT-TTF)<sub>2</sub>Cu(NCS)<sub>2</sub>: Strong evidence of a FFLO state, *Phys. Rev. B* **85**, 214514 (2012).

[9] I. J. Lee, P. M. Chaikin, and M. J. Naughton, Exceeding the Pauli paramagnetic limit in the critical field of (TMTSF)<sub>2</sub>PF<sub>6</sub>, *Phys. Rev. B* **62**, R14669 (2000).

[10] E. Bauer, G. Hilscher, H. Michor, C. Paul, E. W. Scheidt, A. Gribanov, Y. Seropogin, H. Noël, M. Sigrist, and P. Rogl, Heavy Fermion Superconductivity and Magnetic Order in Noncentrosymmetric CePt<sub>3</sub>Si, *Phys. Rev. Lett.* **92**, 027003 (2004).

[11] N. Kimura, K. Ito, H. Aoki, S. Uji, and T. Terashima, Extremely High Upper Critical Magnetic Field of the Noncentrosymmetric Heavy Fermion Superconductor CeRhSi<sub>3</sub>, *Phys. Rev. Lett.* **98**, 197001 (2007).

[12] K. Hoshi, R. Kurihara, Y. Goto, M. Tokunaga, and Y. Mizuguchi, Extremely high upper critical field in BiCh<sub>2</sub>-based (Ch: S and Se) layered superconductor LaO<sub>0.5</sub>F<sub>0.5</sub>Bi<sub>2-x</sub>Se<sub>x</sub> (x = 0.22 and 0.69), *Scientific reports* **12**, 288 (2022).

[13] S. Foner and E. McNiff, Upper critical fields of layered superconducting NbSe<sub>2</sub> at low temperature, *Physics Letters A* **45**, 429 (1973).

[14] D. E. Prober, R. E. Schwall, and M. R. Beasley, Upper critical fields and reduced dimensionality of the superconducting layered compounds, *Phys. Rev. B* **21**, 2717 (1980).

[15] K. Maki and T. Tsuneto, Pauli paramagnetism and superconducting state, *Progress of Theoretical Physics* **31**, 945 (1964).

[16] R. A. Klemm, A. Luther, and M. R. Beasley, Theory of the upper critical field in layered superconductors, *Phys. Rev. B* **12**, 877 (1975).

[17] J. M. Lu, O. Zheliuk, I. Leermakers, N. F. Q. Yuan, U. Zeitler, K. T. Law, and J. T. Ye, Evidence for two-dimensional Ising superconductivity in gated MoS<sub>2</sub>, *Science* **350**, 1353 (2015).

[18] C. Uher, J. L. Cohn, and I. K. Schuller, Upper critical field in anisotropic superconductors, *Phys. Rev. B* **34**, 4906 (1986).

[19] V. Berezinskii, New model of the anisotropic phase of superfluid <sup>3</sup>He, *Jetp Lett.* **20**, 287 (1974).

[20] F. S. Bergeret, A. F. Volkov, and K. B. Efetov, Enhancement of the Josephson Current by an Exchange Field in Superconductor-Ferromagnet Structures, *Phys. Rev. Lett.* **86**, 3140 (2001).

[21] Y. Tanaka, A. A. Golubov, S. Kashiwaya, and M. Ueda, Anomalous Josephson Effect between Even- and Odd-Frequency Superconductors, *Phys. Rev. Lett.* **99**, 037005 (2007).

[22] Y. Asano, A. A. Golubov, Y. V. Fominov, and Y. Tanaka, Unconventional Surface Impedance of a Normal-Metal Film Covering a Spin-Triplet Superconductor Due to Odd-Frequency Cooper Pairs, *Phys. Rev. Lett.* **107**, 087001 (2011).

[23] S.-I. Suzuki and Y. Asano, Paramagnetic instability of small topological superconductors, *Phys. Rev. B* **89**, 184508 (2014).

- [24] A. M. Black-Schaffer and A. V. Balatsky, Odd-frequency superconducting pairing in multiband superconductors, *Phys. Rev. B* **88**, 104514 (2013).
- [25] Y. Asano and A. Sasaki, Odd-frequency Cooper pairs in two-band superconductors and their magnetic response, *Phys. Rev. B* **92**, 224508 (2015).
- [26] A. Ramires, D. F. Agterberg, and M. Sigrist, Tailoring  $T_c$  by symmetry principles: The concept of superconducting fitness, *Phys. Rev. B* **98**, 024501 (2018).
- [27] C. Triola, J. Cayao, and A. M. Black-Schaffer, The Role of Odd-Frequency Pairing in Multiband Superconductors, *Annalen der Physik* **532**, 1900298 (2020).
- [28] P. A. Frigeri, D. F. Agterberg, and M. Sigrist, Spin susceptibility in superconductors without inversion symmetry, *New Journal of Physics* **6**, 115 (2004).
- [29] K. Yamaki and Y. Asano, Singlet/triplet Josephson junction on a substrate, *Phys. Rev. B* **111**, 214505 (2025).
- [30] G. Sarma, On the influence of a uniform exchange field acting on the spins of the conduction electrons in a superconductor, *Journal of Physics and Chemistry of Solids* **24**, 1029 (1963).
- [31] T. Sato, S. Kobayashi, and Y. Asano, Discontinuous transition to a superconducting phase, *Phys. Rev. B* **110**, 144503 (2024).
- [32] N. F. Q. Yuan and L. Fu, Topological metals and finite-momentum superconductors, *Proceedings of the National Academy of Sciences* **118**, e2019063118 (2021).